A Novel Pyramidal Dual-Tree Directional Filter Bank Domain Color Image Watermarking Algorithm*

Panpan Niu[1,**], Xiangyang Wang[2], and Mingyu Lu[1]

[1] School of Information Science & Technology, Dalian Maritime University, Dalian, 116026, China
[2] School of Computer & Information Technology, Liaoning Normal University, Dalian 116029, China
niupanpan3333@yahoo.com.cn, wxy37@126.com

Abstract. Geometric distortion is known as one of the most difficult attacks to resist, for it can desynchronize the location of the watermark and hence causes incorrect watermark detection. It is a challenging work to design a robust color image watermarking scheme against geometric distortions. Based on the Support Vector Regression (SVR) and Pyramidal Dual-Tree Directional Filter Bank (PDTDFB), a new color image watermarking algorithm against geometric distortion is proposed. Experimental results show that the proposed scheme is not only invisible and robust against common image processing operations such as median filtering, noise adding, and JPEG compression etc., but also robust against the geometrical distortions and combined attacks.

Keywords: Color image watermarking, geometric distortion, pyramidal dual-tree directional filter bank (PDTDFB), support vector regression (SVR).

1 Introduction

In recent years, there is an unprecedented development in the robust image watermarking field [1]. However, numerous watermarking schemes have been proposed and applied for gray images. Several existing watermarking schemes for color images are robust to common signal processing, but show severe problems to geometric distortion. Even a slight geometric distortion may significantly influence the extraction of watermark because the synchronization of the watermark is destroyed. Hence, it is a challenging work to design a robust color image watermarking scheme against geometrical distortions.

Nowadays, several approaches that counterattack geometric distortions for color images have been developed. These schemes can be roughly divided into invariant transform, template insertion and feature-based algorithms [2]-[3].

* This work was supported by the National Natural Science Foundation of China under Grant No. 60873222 & 61073133, and Liaoning Research Project for Institutions of Higher Education of China under Grant No. L2010230.
** Corresponding author.

S. Qing et al. (Eds.): ICICS 2011, LNCS 7043, pp. 158–172, 2011.

Invariant transform: The most obvious way to achieve resilience against geometric distortions for color images is to use an invariant transform. In[4]-[5], the watermark is embedded in an affine-invariant domain by using Multidimensional Fourier transform, generalized Radon transform, QSVD transform, and geometric moments respectively. Tsui *et al*. [6] encodes the $L^*a^*b^*$ components of color images and watermarks are embedded as vectors by modifying the Spatiochromatic Discrete Fourier Transform (SCDFT) coefficients and using the Quaternion Fourier Transform (QFT). Jiang et al. [7] transferred the color host image into hypercomplex frequency domain and selected some real parts of the hypercomplex frequency spectra of the color host image. Despite that they are robust against common signal processing, those techniques involving invariant domain suffer from implementation issues and are vulnerable to global affine transformations.

Template insertion: Another solution to cope with geometric distortions for color images is to identify the transformation by retrieving artificially embedded references. Fu *et al.* [8] presented a novel oblivious color image watermarking scheme based on Linear Discriminant Analysis (LDA). Jiang *et al*. [9] proposed a new watermarking scheme based on the multi-channel image watermarking framework, which generates a watermarking template from one of image channels data. However, this kind of approach can be tampered with by the malicious attack. As for random bending attacks, the template-based methods will be incompetent to estimate the attack parameters. Furthermore, the volume of watermark data is lesser.

Feature-based: The last category that counterattacks geometric distortions for color images is based on media features. Its basic idea is that, by binding the watermark with the geometrically invariant image features (Local Feature Region, LFR) [10], the watermark detection can be done without synchronization error. In [11], the steady color image feature points are extracted by using multi-scale Harris-Laplace detector, and the LFRs are ascertained adaptively according to the feature scale theory. However, some drawbacks indwelled in current feature-based schemes for color images restrict the performance of watermarking system. Firstly, the feature point extraction is sensitive to image modification. Secondly, the fixed value is used to determine the size of LFR so that the watermarking scheme is vulnerable to the scale change of the image. Thirdly, the current feature-based watermarking has not constructed the invariant region of LFR, which lower the robustness against local geometric attacks.

In order to effectively resolve the problem of resisting geometric distortions, the support vector machine (SVM) theory is introduced to the color image watermarking domain [12]-[13]. Wang et al. [14] propose a robust image watermarking algorithm against geometric distortions. In watermark detection, according to the high correlation among subimages, the digital watermark can be recovered by using SVR technique. Based on a large number of theory analyses and experimental results, we can easily come to the conclusion that it is possible to resist geometric distortions by utilizing the advanced SVM, but the current SVM based image watermarking have shortcomings as follows: (i) They are not very robust against some geometric distortions, such as cropping, mixed attacks etc; (ii) In watermark detection procedure, the original watermark signal is needed, so it is unfavorable to practical application.

In this paper, a new color image watermarking algorithm with good visual quality and reasonable resistance toward geometric distortions is proposed, in which the Support Vector Regression (SVR) and Pyramidal Dual-Tree Directional Filter Bank (PDTDFB) are utilized.

2 An Introduction to Pyramidal Dual-Tree Directional Filter Bank

The pyramidal dual-tree directional filter bank (PDTDFB) is a new image decomposition, which is recently proposed in [15]. The PDTDFB transform has the following advantages: multiscale and multidirectional transform, efficient implementation, high angular resolution, low redundant ratio, shiftable subbands, and provide local phase information. For the PDTDFB transform, the image decomposition implemented by a filter bank (FB) consists of a Laplacian pyramid and a pair of directional filter banks (DFBs), designated as primal and dual DFBs. Both DFBs are constructed by a binary-tree of two channel fan FBs. The filters of these FBs are designed to have special phase functions so that the overall directional filters of the dual DFB are the Hilbert transforms of the corresponding filters in the primal DFB. Therefore, the two DFBs can be viewed as a single FB with complex directional filters producing complex subband images, whose real and imaginary parts are the outputs of the primal and dual DFB, respectively. A multiresolution representation is obtained by reiterating the decomposition at the lowpass branch. It is shown in [15] that if the lowpass filters used in the Laplacian pyramid have bandpass regions restricted in $[-\pi/2,\pi/2]^2$, then the complex directional subbands at all scale are shiftable.

The object of combining the Laplacian pyramid and dual-tree DFB is to provide a FB that is multiresolution and multidirectional at the same time. However, the Laplacian pyramid structure is not essential to the shiftability of the overall FB. In fact, we can combine any shiftable two-channel 2-D multiresolution FB with the dualtree DFB to obtain an overall shiftable FB. Moreover, it can be shown that the synthesis side of the Laplacian pyramid structure is suboptimal. In this paper, we utilized the construction of a shiftable FB by combining the dual-tree DFBs with a multiresolution FB as in Fig. 1. The advantage of the shiftable FB is that it provides an approximately tight-frame decomposition, which is a desirable property in an overcomplete decomposition. However, the FB is no longer exactly perfect reconstruction and the pyramidal filters are nonseparable.

The new structure for the PDTDFB is illustrated in Fig. 1. The input image is first pass through a two-channel undecimated FB. The filters satisfy perfect reconstruction (PR) condition:

$$\left|R_0(\omega)\right|^2 + \left|L_0(\omega)\right|^2 = 1 \tag{1}$$

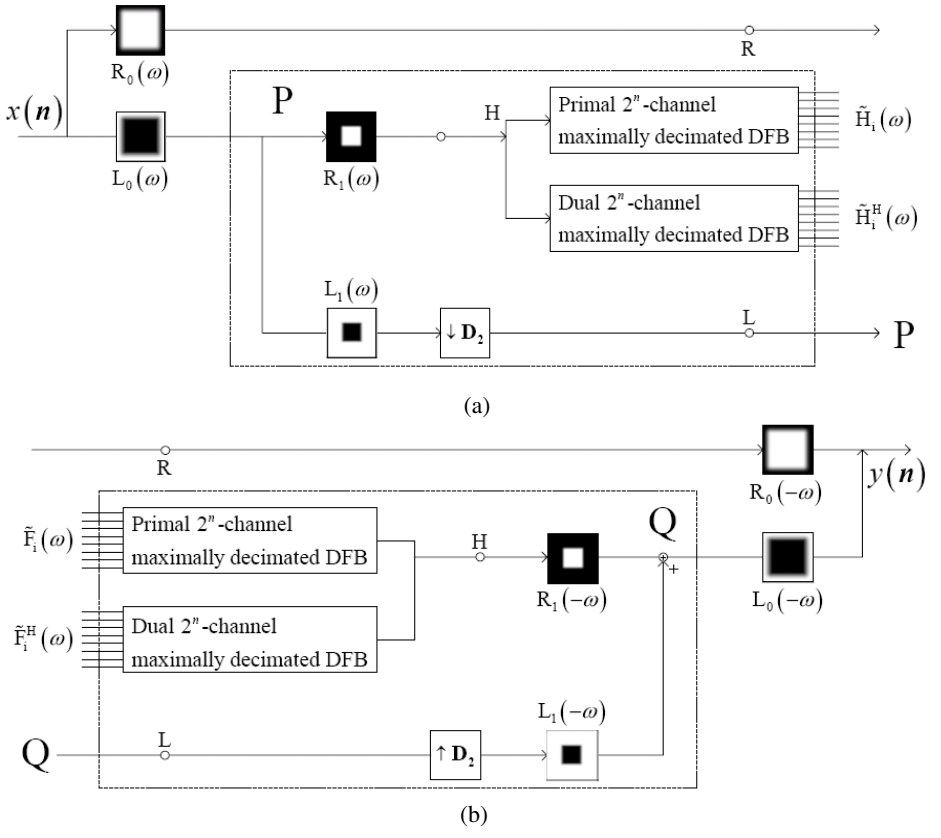

Fig. 1. The PDTDFB structure: (a) analysis side and (b) synthesis side. Blocks P and Q can be reiterated at lower scale for a multiscale representation.

The filter $L_0(\omega)$ is a wide-band lowpass filter while $R_0(\omega)$ is a highpass filter. A slice of the two-dimensional frequency responses of these two filters are in Fig. 2(a). After the undecimated FB, the PDTDFB consists of multiple levels of block P (or Q for the synthesis side) for each scale. This block consists of two filters $R_1(\omega)$ and $L_1(\omega)$ and the dual-tree DFBs. The low frequency component, after filtered by the low-pass filter $L_1(\omega)$ and decimated by $D_2 = 2I$, is fed into the second level decomposition for the second resolution of directional subbands. The filters in blocks P and Q are designed to satisfy the PR and non-aliasing condition (see Fig. 2(b)):

$$|R_1(\omega)|^2 + \frac{1}{4}|L_1(\omega)|^2 = 1 \tag{2}$$

This condition can be approximated by FIR filters. Similar to the Steerable pyramid, the synthesis filters are the time reverse versions of the analysis filters. The design of the PDTDFB can be divided into two parts as follows:

- The design of two-channel FBs, which are used to create multiresolution decomposition. The first is the undecimated two-channel FB with two filters $R_0(\omega)$ and $L_0(\omega)$ (see Fig. 1). The second is the multirate FB with two filters $R_1(\omega)$ and $L_1(\omega)$.
- The design of the fan FBs of the DFBs. Since the design of the conventional DFB has been discussed extensively, for this part we will only focus on the fan FB at the second level of the binary-tree of the dual DFB, which satisfies the phase constraints.

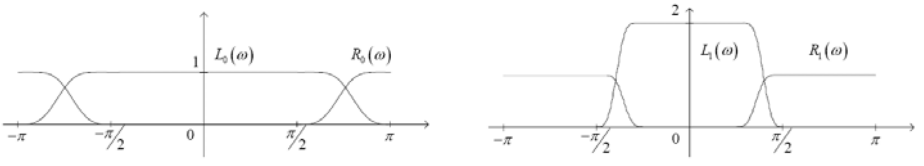

(a) (b)

Fig. 2. A slice of the 2-D frequency responses of (a) $R_0(\omega)$ and $L_0(\omega)$, and (b) $R_1(\omega)$ and $L_1(\omega)$

Each of the two filter design problems above has different design constraints. Since all of these constraints are on the frequency responses, all filters will be designed in frequency domain. In theory, these filters have infinite impulse responses. Sufficiently smooth transition band will be included in order to obtain reasonably short and effective impulse responses. Our approach is to define the ideal filters in frequency domain by using the Meyer function. Then the approximation FIR filters are obtained by truncation of the inverse discrete Fourier transform of the ideal filters. Fig.3. gives experimental results of applying the pyramidal dual-tree directional filter bank (PDTDFB) decomposition with 4 scale and 8 directions on Zoneplate image.

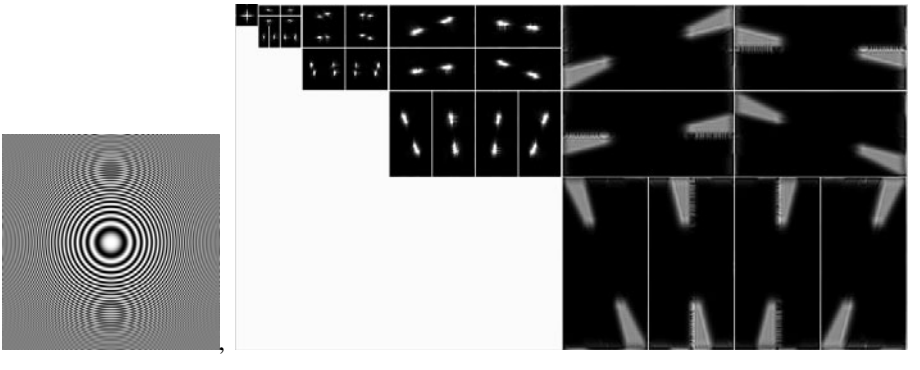

(a) (b)

Fig. 3. The PDTDFB decomposition on Zoneplate image. (a) The Zoneplate image (b) The PDTDFB decomposition result.

The PDTDFB transform has all the nice properties of the contourlet transform, such as multiresolution, multidirectional and low redundancy ratio. Moreover, its subbands are shiftable and provide local phase information. The nonsubsampled contourlet transform [14] also provides shiftable subbands but at the cost of much higher redundant ratio and computational complexity. Therefore, the PDTDFB has been proven to be more efficient in image processing compared to other directional multiresolution transforms.

3 Watermark Embedding Scheme

Based on the above ideas, a new PDTDFB domain color image watermarking algorithm with good visual quality and reasonable resistance toward geometric distortions is proposed. Firstly, the geometrically invariant space is constructed by using color image normalization, and a significant region is obtained from it. Secondly, the PDTDFB transform is performed on the green channel of the significant region, and the digital watermark is embedded into host color image by modifying the low frequency PDTDFB coefficients, in which the HVS masking is used to control the watermark embedding strength.

Let $I = \{f^R(x, y), f^G(x, y), f^B(x, y)\}(0 \le x < M, 0 \le y < N)$ denote a host digital image (color image), and $f^R(x, y), f^G(x, y), f^B(x, y)$ are the color component values at position (x, y).

$W = \{w(i, j), 0 \le i < P, 0 \le j < Q\}$ is a binary image to be embedded within the host image, and $w(i, j) \in \{0,1\}$ is the pixel value at (i, j). The digital watermark embedding scheme can be summarized as follows.

3.1 Watermark Preprocessing

In order to dispel the pixel space relationship of the binary watermark image, and improve the robustness of the whole digital watermark system, the binary watermark image is scrambled from W to W_1 by using Arnold transform. Then, it is transformed into a one-dimensional sequence of ones and zeros as follows:

$$W_2 = \{w_2(k) = w_1(i, j), 0 \le i < P, 0 \le j < Q, k = i \times Q + j, w_2(k) \in \{0,1\}\} \quad (3)$$

3.2 Image Normalization and Significant Region Extraction

In order to improve the robustness against geometrical distortions, we apply the color image normalization on origin host image to produce the standard size normalized image, as shown in Fig. 4(b). The significant region is extracted from the normalized color image by using the invariant centroid, which is more suitable for embedding digital watermark, as shown in Fig.4(c).

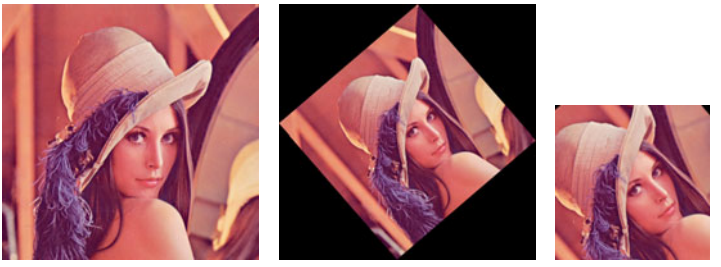

(a) (b) (c)

Fig. 4. The color image normalization and significant region extraction: (a) The color image, (b) The normalized version, (c) The significant region

3.3 The PDTDFB of the Significant Region

When the RGB components of the colored images are visualized separately, the green channel shows the best contrast, whereas the red and blue channels show low contrast and are very noisy. Therefore, the green component of significant region was selected to be embedded watermarking in this paper.

We perform one level PDTDFB decomposition on the green component of significant region, and then obtain the corresponding lowpass subband A.

3.4 Digital Watermark Embedding

Watermark embedding method

The lowpass subband A is divided into 3×3 PDTDFB coefficients blocks A_i $(i=0,1,\cdots,S_1/3\times S_2/3-1)$. By using secret key K_1, $P\times Q$ PDTDFB coefficients blocks are selected from the lowpass subband A. The digital watermark is embedded into the green component of significant region by modifying the selected $P\times Q$ PDTDFB coefficient blocks B_k.

$$b_k'(x+l,y+r)=\begin{cases} b_k(x+l,y+r)+C(x+l,y+r)\cdot S(h^2(B_k)), if\ \ w_2(k)=1 \\ b_k(x+l,y+r)-C(x+l,y+r)\cdot S(h^2(B_k)), if\ \ w_2(k)=0 \end{cases} \quad (4)$$

$$(k=0,1,\cdots,P\times Q-1)\ \ (l=-1,0,1;r=-1,0,1;\mathrm{mod}(l+r,2)=0)$$

where $b_k^{'}(x+l,y+r)$ is the modified PDTDFB coefficients in block B_k, $b_k(x+l,y+r)$ is the original PDTDFB coefficients in block B_k, and $C(x,y)$ is the watermark embedding strength according to the HVS masking of the color image, adaptively. $S(h^2(B_k))$ is the sum of the homogeneity features for all PDTDFB coefficients in block B_k:

$$S(h^2(B_k)) = \sum_{l=-1}^{1}\sum_{r=-1}^{1}(h^2(b_k(x+l, y+r)) \tag{5}$$

In this paper, we employ the concept of the homogeneity [16] to extract homogeneous regions in each PDTDFB coefficient in the lowpass subband A. Assume $b(x, y)$ is the PDTDFB coefficient at the location (x, y) in the lowpass subband A. The homogeneity is represented by:

$$h(b(x, y)) = 1 - E\big(b(x, y), w_m(x, y)\big) \times V\big(b(x, y), w_n(x, y)\big) \tag{6}$$

$$V\big(b(x, y), w_n(x, y)\big) = \frac{\nu(x, y)}{\max\{\nu(x, y)\}},\ E\big(b(x, y), w_m(x, y)\big) = \frac{e(x, y)}{\max\{e(x, y)\}} \tag{7}$$

$e(x, y)$ and $\nu(x, y)$ are the discontinuity and the standard deviation of the coefficient $b(x, y)$ at the location (x, y).

Computing the quantization step

We determine the different mask properties of the human vision system about the luminance, texture and edge of the color host image, and then combine these three masking together to get a comprehensive final masking for the watermark embedding strength $C = M_T - M_E + M_L$. M_L is the luminance masking, M_T is the texture masking, and M_E is the edge masking. The calculations of these three maskings are as follows:

(1) Let $f_A(x, y)$ is the luminance value of the pixel at (x, y), and $\overline{f_A}$ denote the local average luminance value of the pixels within the sliding window of size 5×5:

$$f_A = \sqrt{f_R^2(x, y) + f_G^2(x, y) + f_B^2(x, y)}\ , P_L = (\overline{f_A} - \overline{f_{mid}})^2 \tag{8}$$

where $\overline{f_{mid}}$ is the midst luminance value of the color host image [7]. The calculation of the luminance masking M_L is as follows:

$$M_L = round\left(\frac{8P_L}{\max(P_L)}\right) \tag{9}$$

(2) As for the texture masking, firstly, we use the absolute value of the distance between each pixel and local average value of the pixels within the sliding window as the masking. The size of the sliding window is still 3×3:

$$P_{TCo} = \left|Co(x, y) - \bar{Co}(x, y)\right| \tag{10}$$

$$\bar{Co}(x,y)=\frac{1}{(2L+1)^2}\sum_{k=-L}^{L}\sum_{l=-L}^{L}Co(x+k,y+l) \tag{11}$$

where, $Co(x,y)$ is the color component values at position (x,y), $Co=\{R,G,B\}$. P_{TCo} denote the texture masking of each color channel, and $(2L+1)^2$ represents the number of pixels in the image block[17].

Then, we calculate the average value of the texture masking of three color channels and the calculation of M_T is as follows:

$$P_T=\frac{1}{3}\left(P_{TR}+P_{TG}+P_{TB}\right), M_T=round\left(\frac{8P_T}{\max(P_T)}\right) \tag{12}$$

(3) The way to create edge masking is using Canny's algorithm and the dilated edge detection. Canny's algorithm is good at detecting the weak edges. The dilated edge detection of the image can be used as a filter to wipe off the non-edge regions in the edge masking derived from the Laplacian filter and to only keep the edge areas. The calculation of the edge masking M_E is as follows:

$$P_E=E_{D2}(E_{D1}(I)), M_E=round\left(\frac{8P_E}{\max(P_E)}\right) \tag{13}$$

where I is the original image, $E_{D1}(\cdot)$ is the edge detection operation, and $E_{D2}(\cdot)$ is the dilation operation.

3.5 Obtaining the Watermarked Color Image

Firstly, the watermarked green component of significant region can be obtained by performing the inverse PDTDFB transform with the modified lowpass PDTDFB coefficients. Secondly, the watermarked significant region of the normalized color image can be obtained by combining the watermarked green component, and original red component and blue component. Finally, we can obtain the watermarked color image by performing the inverse color image normalization with the watermarked significant region.

4 Watermark Detection Scheme

According to the high correlation among different channels of the color image, a robust color image watermarking detection algorithm based on support vector regression (SVR) [18] is proposed, which neither needs the original host color image nor any other side information. The main steps of the watermark detecting procedure developed can be described as follows.

4.1 Image Normalization and Significant Region Extraction

Color image normalization is applied on the watermarked color image I^* to produce the standard size normalized image. The significant region is extracted from the normalized watermarked color image by using the invariant centroid.

4.2 The PDTDFB of the Significant Region

After one level PDTDFB decomposition has been applied on red component and green component of significant region, the corresponding lowpass subbands RA^* and GA^* are obtained.

4.3 Selecting the Embedded Position

The lowpass subbands RA^* and GA^* are divided into 3×3 PDTDFB coefficients blocks RA_i^* and GA_i^* $(i=0,1,\cdots,S_1/3\times S_2/3-1)$. By using the same secret key K_1, $P\times Q$ PDTDFB coefficients blocks RB_k^* and GB_k^* $(k=0,1,\cdots,P\times Q-1)$ are selected from RA_i^* and GA_i^*, respectively. Here, the PDTDFB coefficients RB_{k1}^* and GB_{k1}^* are used for training the SVR model, and the other PDTDFB coefficients RB_{k2}^* and GB_{k2}^* are used for extracting digital watermark.

$$CB_{k1}^*=\{b_k^C(x+l,y),b_k^C(x,y+r),l=-1,1,r=-1,1,k=0,1,\cdots,P\times Q-1\}\ (C\in\{R,G\}) \quad (14)$$

$$CB_{k2}^*=\{b_k^C(x,y),b_k^C(x+l,y+r),l=-1,1,r=-1,1,k=0,1,\cdots,P\times Q-1\}\ (C\in\{R,G\}) \quad (15)$$

4.4 SVR Training

Let $S(h^2(B_{k1}))$ (see equation (5)) be the sum of the homogeneity features for all PDTDFB coefficients in block RB_{k1}^*, and RV_{k1}^* be the average value of a part of the coefficients in block RB_{k1}^*:

$$RV_{k1}^*=\frac{1}{4}\left(\sum_{l=-1}^{1}b_k^R(x+l,y)+\sum_{r=-1}^{1}b_k^R(x,y+r)-2b_k^R(x,y)\right) \quad (16)$$

In the same way, GV_{k1}^* is the average value of a part of the coefficients in block GB_{k1}^*.

Then, let RV_{k1}^* and $S(h^2(B_{k1}))$ be the feature vectors for training, and GV_{k1}^* be the training objective. We can obtain the training samples as following:

$$\Omega_k^* = \left\{GV_{k1}^*, RV_{k1}^*, S(h^2(RB_{k1}))\right\} (k = 0,1,\cdots, P\times Q-1)$$

So, the SVR model can be obtained by training.

4.5 Digital Watermark Extracting

Let $S(h^2(B_{k2}))$ (see equation (5)) be the sum of the homogeneity features for all PDTDFB coefficients in block RB_{k2}^*. RV_{k2}^* is the average value of a part of the coefficients in block RB_{k2}^*:

$$RV_{k2}^* = \frac{1}{5}\left(\sum_{l=-1}^{1} b_k^R(x+l, y+l) + \sum_{r=-1}^{1} b_k^R(x-r, y+r) - b_k^R(x,y)\right) \tag{17}$$

Let RV_{k2}^* and $S(h^2(B_{k2}))$ be the input vector.

Then, the actual output vector $\overline{GV}_{k2}^*$ can be obtained by using the well trained SVR model. The digital watermark $w_2^*(k)$ can be extracted by comparing the actual output vector $\overline{GV}_{k2}^*$ with the GV_{k2}^* (GV_{k2}^* is the average value of a part of the coefficients in block GB_{k2}^*), and the rule of extracting digital watermark can be described

$$w_2^*(k) = \begin{cases} 1, & if \quad GV_{k2}^* > \overline{GV}_{k2}^* \\ 0, & else \end{cases}, (k = 0,1,\cdots, P\times Q-1) \tag{18}$$

4.6 Watermark Postprocessing

All the detected watermark bits $w_2^*(k)$ are rearranged to form the binary watermark image W_1^*, and the watermark image $W^* = \{w^*(i,j), 0 \le i < P, 0 \le j < Q\}$ can be obtained by descrambling.

5 Simulation Results

We test the proposed watermarking scheme on the popular 24bit true color images 512×512 Lena, Mandrill, and Barbara, and a 32×32 binary image is used as the digital watermark, as shown in Fig.5. The size of the significant region is $S_1 = S_2 = 256$, the number of training sample is 3072, and the radius-based function (RBF) is selected as the SVR kernel function, and other parameters are set respectively to γ=0.125, C=78. Besides, the PSNR (Peak Signal-to-Noise Ratio) is used to measure the visual quality of the watermarked images. Finally, experimental results are compared with schemes in [14] [19] and [8].

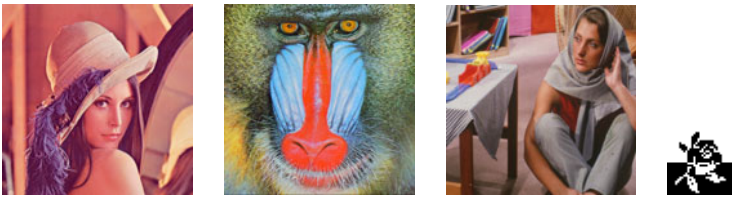

(a) (b) (c) (d)

Fig. 5. The test images and digital watermark: (a) The test image Lena, (b) The test image Mandrill, (c) The test image Barbara, (d) The digital watermark

5.1 Performance Test

As shown in Fig.6, (a), (b) and (c) are the watermarked color images (Lena, Mandrill, and Barbara) and the extracted watermarks obtained by using the proposed scheme. The transparency comparison results in terms of PSNR listed in Table 1 clearly show that proposed method outperforms other three methods.

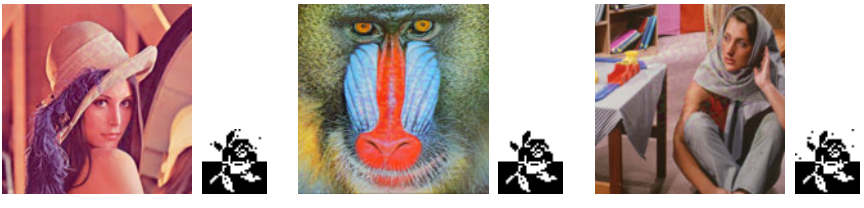

(a) (b) (c)

Fig. 6. The watermarked color images and the extracted watermarks obtained by the proposed scheme: (a) Lena (PSNR=40.32dB, BER=0.0078), (b) Mandrill (PSNR=40.01dB, BER=0), (c) Barbara (PSNR=40.34dB, BER=0.0088)

Table 1. The performance test for different color image watermarking scheme

Test image		Our method	Scheme [14]	Scheme [19]	Scheme [8]
Lena	BER	0.0078	0.0166	0.0098	0.0186
	PSNR(dB)	40.32	41.93	39.43	38.11
Mandrill	BER	0	0.0020	0.0146	0.0889
	PSNR(dB)	40.01	41.67	38.54	38.91
Barbara	BER	0.0088	0.0176	0.0107	0.0430
	PSNR(dB)	40.34	40.71	38.53	39.72

5.2 Performance Test

In order to test the robustness of the proposed scheme, we have done extensive experiments. In this study, reliability was measured as the bit error rate (BER) of extracted watermark. Fig.7, Fig.8 and Fig.9 show the results of comparison with scheme [14] [19] and [8].

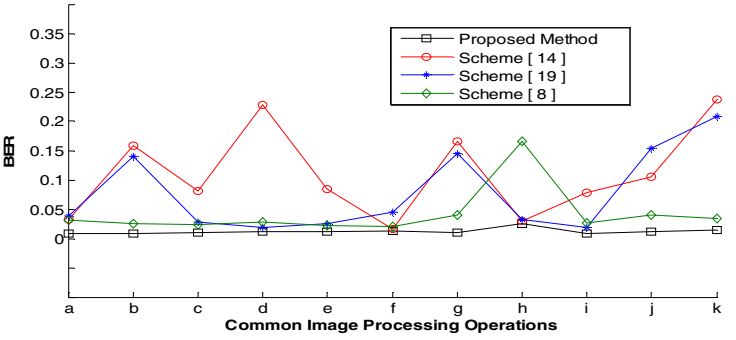

Fig. 7. The watermark detection results for common image processing operations(Lena): (a) Gaussian filtering (3×3), (b) Wiener filtering, (c) Salt and peppers noise (0.01), (d) Speckle noise （0.03, (e) Sharpening, (f) Histogram equalization, (g) Blurring, (h) Gamma correction, (i) JPEG90, (j) JPEG70, (k) JPEG50

Common image processing operations: Traditional signal processing attacks affect watermark detection by reducing the watermark energy. Fig.7 shows the quantitative results for the common image processing operations. It is evident that our scheme is more robust against wiener filtering, histogram equalization, blurring, gamma correction etc., compared with scheme [14] [19] and [8].

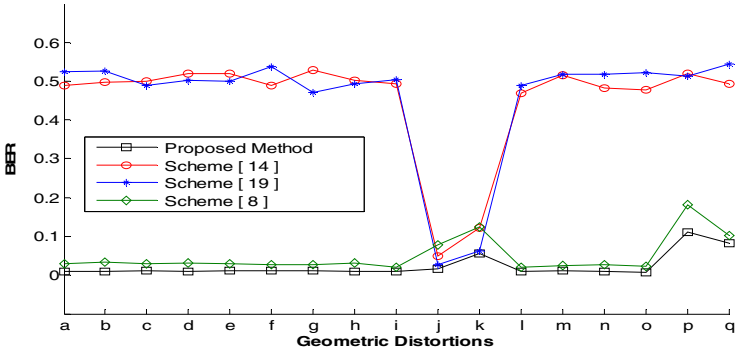

Fig. 8. The watermark detection results for geometric attacks(Lena): (a) Rotation 5°, (b) Rotation 45°, (c) Rotation 70°, (d) Scaling 1.2, (e) Scaling 1.5, (f) Scaling 2, (g) Translation(H 20,V 20), (h) Translation(H 15,V 5), (i) Translation(H 0,V 50), (j) Cropping 10%, (k) Cropping 30%, (l) Length- width ratio change(1.1,1.0), (m) Length-width ratio change(1.2,1.0), (n) Affine Transformation[5; 1.0, 1.0; 0.3, 0.1], (o) Affine Transformation[10; 1.0, 1.0; 0.5, 0.2], (p) Flip Horizontally, (q) Flip Vertically

Geometric distortions: Our scheme can resist RST attacks and it can extract the watermarks directly from the watermarked color images without any auxiliary operations. Fig.8 shows the quantitative results for the geometric distortions, respectively. From these quantity results, it is verified that our scheme yields better robustness than those in scheme [14] [19] and [8].

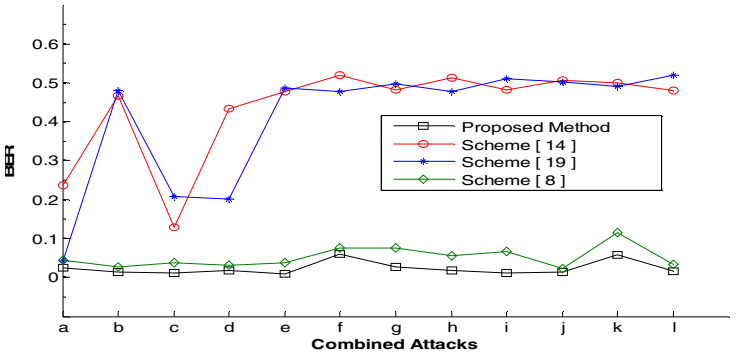

Fig. 9. The watermark detection results for combined attacks(Lena): (a) Gaussian Noise (0.05)+Sharpening, (b) Median Filtering (3×3) + JPEG70, (c) Sharpening+JPEG70, (d) Salt and Peppers Noise (0.01) + Gaussian Filtering (3×3)+JPEG70, (e) Rotation 15°+Scaling1.2, (f) Scaling1.2+Translation(H 5,V15), (g) Rotation 15° +Cropping10%, (h) Rotation 45°+Translation (H 20,V20)+Scaling1.2, (i) Rotation 5° + Median Filtering (3×3), (j) Scaling1.2+ Gaussian Noise(0.05), (k) Translation(H5,V15)+Salt and Peppers Noise(0.01), (l) Affine Transformation[-10; 1.0, 1.0; -0.5, -0.2]+JPEG50

Combined attacks: Except for individual attack, we also conduct some attacks that combine two or more kind of attacks. The combined attacks include median filtering plus Gaussian noise, rotation plus scaling plus translation, affine transformation plus JPEG compression etc. Fig.9 provides the quantitative results for the combined attacks, respectively. It is verified that our scheme yields better robustness than those in scheme [14] [19] and [8].

To sum up, the proposed scheme can efficiently resist common image processing operations, geometric distortions and combined attacks. Comparisons show that the overall performance of our scheme is superior to the existing schemes.

6 Conclusion

This paper presents a blind color image watermarking algorithm by using the Support Vector Regression (SVR) and Pyramidal Dual-Tree Directional Filter Bank (PDTDFB). The extensive experimental works have shown that the proposed color image watermarking has conquered those challenging geometric distortions, such as rotation, translation, scaling, and length-width ratio change etc. Also, the digital watermark can resist some common image processing operations, the geometric distortions and combined attacks.

References

1. Lian, S., Kanellopoulos, D., Ruffo, G.: Recent advances in multimedia information system security. Informatica 33, 3–24 (2009)
2. Zheng, D., Liu, Y., Zhao, J.Y., Saddik, A.E.: A survey of RST invariant image watermarking algorithms. ACM Computing Surveys 39, 1–91 (2007)

3. Zheng, D., Wang, S., Zhao, J.Y.: RST invariant image watermarking algorithm with mathematical modeling and analysis of the watermarking processes. IEEE Trans. on Image Processing 18, 1055–1068 (2009)
4. Lin, S.D., Shie, S.C., Guo, J.Y.: Improving the robustness of DCT-based image watermarking against JPEG compression. Computer Standards & Interfaces 32, 54–60 (2010)
5. Xing, Y., Tan, J.: A color image watermarking scheme resistant against geometrical attacks. Radio Engineering 19, 62–67 (2010)
6. Kin, T.T., Zhang, X.P., Androutsos, D.: Color Image Watermarking Using Multidimensional Fourier Transforms. IEEE Trans. on Information Forensics and Security 3, 16–28 (2008)
7. Jiang, S.H., Zhang, J.Q., Hu, B.: An adaptive watermarking algorithm in the hypercomplex space of a color image. Acta Electronica Sinica 37, 1773–1778 (2009)
8. Fu, Y.G., Shen, R.M.: Color image watermarking scheme based on linear discriminant analysis. Computer Standard & Interfaces 30, 115–120 (2008)
9. Zheng, J.B., Feng, S.: A Color Image Watermarking Scheme in the Associated Domain of DWT and DCT Domains Based on Multi-channel Watermarking Framework. In: Kim, H.-J., Katzenbeisser, S., Ho, A.T.S. (eds.) IWDW 2008. LNCS, vol. 5450, pp. 419–432. Springer, Heidelberg (2009)
10. Liu, K.C.: Wavelet-based watermarking for color images through visual masking. AEU - International Journal of Electronics and Communications 64, 112–124 (2010)
11. Wang, X.Y., Meng, L., Yang, H.Y.: Geometrically invariant color image watermarking scheme using feature points. Science in China Series F-Information Sciences 52, 1605–1616 (2009)
12. Wang, X.Y., Xu, Z.H., Yang, H.Y.: A robust image watermarking algorithm using SVR detection. Expert Systems with Applications 36, 9056–9064 (2009)
13. Tsai, H.H., Sun, D.W.: Color image watermark extraction based on support vector machines. Information Sciences 177, 550–569 (2007)
14. Niu, P.P., Wang, X.Y., Yang, Y.P., Lu, M.Y.: A novel color image watermarking scheme in nonsampled contourlet-domain. Expert Systems with Applications 38, 2081–2098 (2011)
15. Nguyen, T.T., Oraintara, S.: The shiftable complex directional pyramid-part I: theoretical aspects. IEEE Trans. on Signal Processing 56, 4651–4660 (2008)
16. Chaabane, S.B., Sayadi, M., Fnaiech, F.: Colour image segmentation using homogeneity method and data fusion techniques. EURASIP Journal on Advances in Signal Processing, 1–11 (2010)
17. Qi, H.Y., Zheng, D., Zhao, J.Y.: Human visual system based adaptive digital image watermarking. Signal Processing 88, 174–188 (2008)
18. Vapnik, V.: The nature of statistical learning theory. Springer, New York (1995)
19. Peng, H., Wang, J., Wang, W.X.: Image watermarking method in multiwavelet domain based on support vector machines. Journal of Systems and Software 83, 1470–1477 (2010)